RESEARCH ARTICLE

The Proteome of the Locus Ceruleus in Parkinson's Disease: Relevance to Pathogenesis

Karin D. van Dijk[1,2]; Henk W. Berendse[2]; Benjamin Drukarch[1]; Silvina A. Fratantoni[3]; Thang V. Pham[3]; Sander R. Piersma[3]; Evelien Huisman[1]; John J.P. Brevé[1]; Henk J. Groenewegen[1]; Connie R. Jimenez[3]*; Wilma D.J. van de Berg[1]*

[1] Department of Anatomy and Neurosciences, Section Functional Neuroanatomy, Neuroscience Campus Amsterdam, VU University Medical Center Amsterdam, the Netherlands.
[2] Department of Neurology, Neuroscience Campus Amsterdam, VU University Medical Center Amsterdam, the Netherlands.
[3] OncoProteomics Laboratory of the Department of Medical Oncology, VU University Medical Center Amsterdam, the Netherlands.

Corresponding author:

Karin D. van Dijk, MD, Department of Anatomy and Neurosciences, Section Functional Neuroanatomy, Neuroscience Campus Amsterdam, VU University Medical Center Amsterdam, PO Box 7057, 1007 MB Amsterdam, the Netherlands (E-mail: *karin.vandijk@vumc.nl*)

* CRJ and WDJB contributed equally to the coordination of the work

Abstract

The locus ceruleus is among the earliest affected brain regions in Parkinson's disease (PD) showing Lewy body pathology and neuronal loss. To improve our understanding of the pathogenesis of PD, we performed the first proteomic analysis ever of post-mortem locus ceruleus tissue of six pathologically confirmed PD patients, and six age- and gender-matched non-neurological controls. In total 2495 proteins were identified, of which 87 proteins were differentially expressed in the locus ceruleus of PD patients compared with controls. The majority of these differentially expressed proteins are known to be involved in processes that have been implicated in the pathogenesis of PD previously, including mitochondrial dysfunction, oxidative stress, protein misfolding, cytoskeleton dysregulation and inflammation. Several individual proteins were identified that have hitherto not been associated with PD, such as regucalcin, which plays a role in maintaining intracellular calcium homeostasis, and isoform 1 of kinectin, which is involved in transport of cellular components along microtubules. In addition, pathway analysis suggests a pathogenetic role for aminoacyl-tRNA-biosynthesis. These findings indicate that the proteome of the locus ceruleus of PD patients and non-neurological controls provides data that are relevant to the pathogenesis of PD, reflecting both known and potentially novel pathogenetic pathways.

INTRODUCTION

Parkinson's disease (PD) is neuropathologically characterized by intraneuronal protein aggregates called Lewy bodies. Lewy body pathology within the central nervous system coincides with neuronal loss and affects specific brain regions in a predictive caudal to rostral order, ascending from the lower brainstem to neocortical areas (14). The underlying pathogenetic mechanisms have not yet been fully clarified, although several processes have been implicated. Both genetic studies and post-mortem analyses of substantia nigra tissue are in support of an important role of mitochondrial dysfunction, oxidative stress and inflammation in PD pathogenesis (24, 46), whereas impaired protein degradation and apoptosis-mediated cell death appear to be other major pathogenetic factors (55).

The necessity to further improve our understanding of the pathogenetic mechanisms underlying PD results from the current lack of an effective causal treatment. Until now, the treatment of PD is largely limited to symptomatic dopaminergic substitution therapy.

Increased insight into pathogenetic pathways and cellular processes involved in PD pathology is a prerequisite for the development of disease-modifying therapeutic strategies. Important sources of diagnostic biomarkers or therapeutic targets are proteins, which are abundantly present in brain tissue and likely reflect disturbed brain mechanisms. The recent application of proteomics—a protein profiling technique that enables to study disease mechanisms in an unbiased way—has already revealed additional proteins and molecular mechanisms involved in PD pathogenesis, such as cytoskeletal dysregulation and neuronal plasticity (2, 35). So far, the rare comparative proteomic studies of post-mortem brain tissue in PD patients have been confined to substantia nigra and frontal cortical regions (7, 8, 25, 30, 49, 50, 56). Tissue proteomic analyses of potentially interesting early-affected brain regions have, as yet, not been described.

One of the early-affected brain regions in PD is the locus ceruleus (LC), which may already be involved in preclinical stages of the disease, that is, before the appearance of the characteristic motor symptoms (14). The average loss of noradrenergic neurons

in this region is around 70% in post-mortem brain tissue of PD patients compared with controls (10). The LC is the principal site for the synthesis of noradrenaline and its neurons extensively project to the entire brain (21). It is functionally related to arousal, autonomic function and cognition (45, 58). The involvement of the LC in PD may therefore contribute to some of the prodromal non-motor symptoms, in particular sleep disorders and autonomic dysfunction. Neuronal loss in the LC is not specific for PD. It can also be observed in other neurological disorders, including Alzheimer's disease (AD) and multiple system atrophy (MSA) (9, 20).

In the present study, we performed the first proteomic analysis on human post-mortem LC tissue to date. By profiling the LC proteomes of PD patients and comparing them with non-neurological controls, we aimed to identify proteins and processes that are involved in the pathogenesis of PD. In particular, we intended to identify novel pathogenetic mechanisms.

MATERIALS AND METHODS

Post-mortem human LC tissue

Snap-frozen post-mortem LC tissue of six PD patients and six non-neurological controls was obtained from the Netherlands Brain Bank (NBB; Amsterdam, the Netherlands). All donors gave written informed consent for brain autopsy and the subsequent use of their brains for research purposes. To ensure high quality post-mortem tissue, only cases with a post-mortem interval less than 12 h and a pH of ventricular cerebrospinal fluid between 6.3 and 7.1 were included. Only females were included, to have more homogeneous groups. PD patients were clinically and pathologically diagnosed with PD or PD dementia and had no history of cancer or concomitant disease of the central nervous system. The controls had no history of cancer, psychiatric or central nervous system diseases, and their neuropathological examinations revealed age-related changes only. PD patients and controls were matched for age [mean ± standard deviation (SD) for PD 77.8 ± 4.4 years, for controls 77.8 ± 5.7 years; $P = 1.0$], post-mortem interval (mean ± SD for PD 5:46 ± 2:20 h, for controls 7:09 ± 2:31 h; $P = 0.35$) and pH of ventricular cerebrospinal fluid (mean ± SD for PD 6.69 ± 0.19, for controls 6.75 ± 0.27; $P = 0.67$). The brainstem was dissected at the level of the inferior cerebral peduncles and directly caudally to the pons and cut into a right and left half. The left side of the brain stem including the LC was frozen in liquid nitrogen and stored at −80°C until further processing. In both PD patients and controls the presence and distribution of alpha-synuclein and tangle pathology was evaluated and staged according to Braak (13, 14) and the BrainNet Europe protocol (1). Amyloid pathology was staged according to the Consortium to Establish a Registry for Alzheimer's Disease (CERAD) criteria (36). For immunohistochemical validation, we included two additional PD patients, one additional control and four AD patients. AD patients were clinically and pathologically diagnosed with AD and were included to evaluate the specificity of our findings. See Table 1 for the clinical and neuropathological characteristics of the included cases.

Tissue dissection

Accurate dissection of the LC is essential to acquire useful proteomic data of this nucleus. Including non-affected neighbouring tissue would reduce the fold change of differential proteins in the affected LC itself. In the current study we were able to accurately dissect the LC by a punch technique in a −20°C cryostat. With a 3-mm punch, the LC was marked and a 20 μm thick section was made to microscopically verify whether the neuromelanin-containing neurons of the LC were located within the punch. When all neuromelanin-containing neurons of the LC were inside the punch, thicker sections were made and punches were collected in Eppendorf tubes. The punches were collected throughout the entire available nucleus, ranging from 4 to 16 mm. Sections for microscopic evaluation were made every 1.2 mm to verify the location of the punch.

Sample preparation

The punched LC of each case was homogenized in 300 μL sample buffer [50 mM Tris-HCl pH 6.8, 8% glycerol, 1.6% sodium dodecyl sulfate (SDS), 0.002% bromophenol blue, 0.1 M dithiothreitol (DTT)] per approximately 10 mg of tissue. Samples were subsequently denatured by boiling for 5 minutes, centrifuged to remove insoluble fractions and 1.5 times diluted in sample buffer. Two samples were diluted two times in sample buffer (NBB94-092 and NBB03-040) and one sample was diluted three times (NBB98-064), because of protein overloading on the gel using higher concentrations. The different dilutions did not affect the subsequent quantification, because the spectral counts were normalized on the sum of the spectral counts per case.

One dimensional gel electrophoresis and in-gel tryptic digestion

In total 28 μL of homogenized and diluted sample per case was separated on 2 NuPAGE® Novex 4–12% Bis-Tris gels (1.5 mm, 10 well; Invitrogen, Carlsbad CA, USA). The gels were stained with Coomassie Brilliant Blue solution (Coomassie Brilliant Blue R B-0630; Sigma, St. Louis MO, USA; 17% ammonium sulfate, 3% phosphoric acid, 34% methanol), fixed with 50% ethanol/3% phosphoric acid, washed with MilliQ and scanned. Tryptic digestion was performed according to Shevchenko *et al* (48). Gels were washed and dehydrated once in 50 mM ammonium bicarbonate (ABC) and twice in 50 mM ABC/50% acetonitrile (ACN). Cysteine bonds were reduced by incubation with 10 mM DTT/50 mM ABC at 56°C for 1 h and alkylated with 50 mM iodoacetamide/50 mM ABC at room temperature (RT) in the dark for 45 minutes. After washing sequentially with ABC and ABC/50% ACN, we sliced the whole gel lane of each case into 10 parts. Gel parts were sliced up into approximately 1-mm cubes and collected in tubes, washed in ABC/ACN and dried in a vacuum centrifuge. Gel cubes were incubated overnight at 23°C with 6.25 ng/mL trypsin and covered with ABC to allow digestion. Peptides were extracted once in 1% formic acid and twice in 5% formic acid/50% ACN. The volume was reduced to 50 μL in a vacuum centrifuge prior to LC-MS analysis.

Nano-LC separation and tandem mass spectrometry (MS/MS)

Peptides were separated by an Ultimate 3000 nano-LC system (Dionex LC-Packings, Amsterdam, the Netherlands) as described in Piersma *et al* (43). Intact peptide MS spectra and MS/MS

Table 1. Clinical and neuropathological characteristics of included PD patients, AD patients and controls. Abbreviations: PD = Parkinson's disease; PDD = Parkinson's disease with dementia; CTRL = control; AD = Alzheimer's disease; PMI = post-mortem interval in hours; CSF = cerebrospinal fluid; NA = not applicable; ND = not determined.

Subject	Diagnosis	PD Braak stage	AD Braak stage	Amyloid load*	Disease duration (years)†	Sex	Age	PMI (h)	pH CSF	Cause of death
NBB06-002	PD	5	2	B	12	F	84	7:25	6.85	Old age and shortness of breath
NBB94-092	PD	4	0	O	4	F	77	9:40	6.86	Euthanasia
NBB98-043	PD	5	1	O	17	F	81	4:10	6.86	Pneumonia
NBB98-064	PDD	6	1	B	16	F	74	4:35	6.5	Pneumonia
NBB99-014	PDD	6	2	B	7	F	72	3:25	6.46	Pneumonia and heart failure
NBB99-069	PD	5	1	O	15	F	79	5:20	6.62	Kidney failure complicated by heart failure
NBB96-078	CTRL	0	2	ND	NA	F	87	8:00	6.91	Heart failure
NBB03-040	CTRL	0	0	B	NA	F	73	4:00	6.47	Pulmonary fibrosis, rhabdomyolysis and progressive renal insufficiency
NBB03-013	CTRL	0	1	O	NA	F	82	11:30	6.77	Congestive heart failure
NBB95-101	CTRL	0	1	O	NA	F	73	5:30	6.38	Cardiac arrest
NBB98-104	CTRL	0	2	A	NA	F	74	7:25	6.95	Intestinal necrosis secondary to thrombosis
NBB00-032	CTRL	0	1	A	NA	F	78	6:30	7.02	Heart failure
Additional subjects included for immunohistochemistry										
NBB07-090	PD	6	2	B	22	F	70	7:05	6.64	Pneumonia
NBB07-008	PD	6	1	B	6	M	80	7:05	6.34	Pneumonia
NBB97-043	CTRL	0	ND	ND	NA	M	68	10:10	7.08	Cardiac arrest
NBB02-050	AD	0	4	B	7	F	95	4:10	6.45	Myocardial infarction
NBB02-021	AD	0	6	C	6	F	64	3:40	6.65	Pneumonia
NBB07-027	AD	0	6	C	2	M	60	6:15	6.58	Dehydration
NBB07-080	AD	0	5	C	3	F	90	5:00	6.36	Unknown

*The load of amyloid was scored according to the Consortium to Establish a Registry for Alzheimer's Disease (CERAD) criteria (41).
†Disease duration in years, starting from timepoint of clinical diagnosis.

spectra were acquired on an LTQ-FT hybrid mass spectrometer (Thermo Fisher, Bremen, Germany) as described previously (3, 43). Intact masses were measured at 50.000 resolution and the top five most intense signals were subjected to collision-induced dissociation (CID) in the linear ion trap.

Protein identification, quantification, statistics, pathway analysis and protein classification

MS/MS spectra were searched against the human International Protein Index (IPI) database 3.59 (80, 128 entries) using Sequest (version 27, rev 12, Thermo Fisher Scientific, San Jose, CA, USA) with a maximum allowed deviation of 10 ppm for the precursor mass and 1 amu for fragment masses. Scaffold 2.02.03 (Proteomesoftware, Portland, OR, USA) was used to organize the gel-slice data and to validate peptide identifications using the PeptideProphet (27, 37) algorithm; only identifications with a probability >95% were retained. Subsequently, the ProteinProphet (27, 37) algorithm was applied to group peptide identifications into protein identifications. Protein identifications with a probability of >99% with two peptides or more in at least one of the samples were retained ($P < 0.01$). For each protein identified, the number of spectral counts (the number of MS/MS spectra associated with an identified protein) was exported to Excel. For quantitative analysis across samples, spectral counts were normalized to the sum of the spectral counts per biological sample. Each sample was separated in 10 fractions that were subjected to nano-LC-MS/MS. Spectral counts for identified proteins in a sample were summed across all fractions for each sample and were normalized to the total sum of spectral counts for that sample (42). This gives the relative spectral count contribution of a protein to all spectral counts in the sample. When comparing different datasets, these normalized spectral counts were used to calculate ratios. In this way, we were able to correct for loading differences between samples. Differential analysis of samples was performed using the beta-binominal test, which takes into account within- and between-sample variations, giving fold-change values and associated *P*-values for all identified proteins (42). Further protein identification and quantification details can be found in (42, 43). Protein cluster analysis of the differentially expressed proteins was performed using hierarchical clustering in R. The protein abundances were normalized to zero mean and unit variance for each individual protein. Subsequently, the Euclidean distance measure was used for protein clustering. The differentially expressed proteins were imported in the online software package Ingenuity Pathway Analysis (Ingenuity IPA, version 8.8, Ingenuity Systems, Redwood City, CA, USA). Pathway analysis was performed with only direct relationships and *P*-values were obtained and adjusted under Benjamini-Hochberg (B-H) multiple testing corrections. Proteins were functionally classified according to the PANTHER classification (http://www.pantherdb.org). They were assigned to hypothesized pathogenetic pathways for PD based on their GO annotation (6) and Entrez Gene information (http://www.ncbi.nlm.nih.gov/gene) and compared with the proteomic data of previous human brain tissue studies in PD (7, 8, 25, 30, 49, 50, 56).

Western blotting

The expression levels of selected proteins were validated using Western blotting in LC homogenates of the six PD patients and six controls that were also included in our proteomic analysis (for the case characteristics see Table 1). The selected proteins were tyrosine hydroxylase (TH), gammabutyrobetaine dioxygenase (BBOX1), phenylalanyl-tRNA synthetase alpha chain (FARSA), isoform 1 of kinectin (KTN1) and complement component C4B (C4B). Total protein amounts were measured with a bicinchoninic acid assay (BCA; Pierce BCA Protein Assay Kit #23225, Thermo Scientific, Rockford IL, USA). Ten micrograms of protein per case were loaded and separated on SDS-12% or SDS-8% polyacrylamide gels under reduced conditions and blotted onto a PVDF membrane (Immobilon, Millipore, Billerica MA, USA). After blockage with 5% (w/v) non-fat dry milk for 30 minutes, the blots were probed with: (i) mouse monoclonal antibody against TH (1:2000, MAB318, Chemicon, Billerica MA, USA); (ii) rabbit polyclonal antibody against BBOX1 (1:250, HPA007600, Atlas Antibodies, Stockholm, Sweden); (iii) rabbit polyclonal antibody against FARSA (1:1000, HPA001911, Atlas Antibodies); (iv) rabbit polyclonal antibody against KTN1 (1:250, HPA003178, Atlas Antibodies); (v) rabbit polyclonal antibody against C4B (1:1000, GTX110502, Genetex, Irvine, CA, USA) or mouse monoclonal antibody against actin (1:200.000, Ab6276, Abcam, Cambridge, MA, USA) overnight at 4°C and incubated for 1 h at RT with horseradish peroxidase-conjugated secondary antibody. Actin was included as a reference protein that should not change in expression level between samples or groups. Actin was loaded on a separate gel because of the overlap of its molecular weight with the other measured proteins. Labeling was detected using a chemiluminescent substrate (Supersignal West Dura #34076, Thermo Scientific) and quantified with Chemidoc XRS Imaging System (Bio-Rad, Hercules CA, USA) and Quantity One Analysis Software (Bio-Rad) after background correction. If more than one band was present, we selected the band that corresponded with the expected molecular weight for quantification. Statistical analysis was performed using unpaired, one-tailed Student's *t*-tests.

Immunohistochemical validation

Immunohistochemical stainings of alpha-synuclein and two selected proteins were performed on paraffin embedded postmortem LC tissue of four PD patients, four controls and four AD patients obtained from the NBB. For this validation we included post-mortem LC tissue of two PD patients (NBB06-002, NBB99-014) and three controls (NBB00-032, NBB03-040, NBB03-013) that were also included in the proteome discovery, with two additional PD patients (NBB07-090, NBB07-008) and one additional non-neurological control (NBB97-043; see Table 1). AD patients were included to evaluate the expression of the two selected proteins in another neurodegenerative disease in which LC neuronal loss occurs, which could inform us about the specificity of our findings.

We focused on one protein of which the level was significantly increased in the LC of PD patients compared with controls, that is, BBOX1, and one protein of which the level was significantly decreased, that is, FARSA. By examining their localizations—guided by the Nissl staining—we aimed to find explanations for the altered levels of these proteins and their relationship to the alpha-synuclein pathology and cell death in the LC.

Ten-micrometer-thick transversal sections were collected throughout the LC using a paraffin microtome (Microm HM340E, Mikron Instruments Inc., San Marcos, CA, USA).

Sections for alpha-synuclein immunostaining were deparaffinized, rehydrated and washed in 95% formic acid, aquadest and Tris-buffered saline (TBS), followed by incubation in 0.3% hydrogen peroxide diluted in ethanol for 15 minutes in order to eliminate endogenous peroxidase activity. Subsequently, the sections were incubated with mouse monoclonal antibody against alpha-synuclein (1:2000, #610786, BD Transduction Laboratories, Franklin Lakes, NJ, USA) diluted in TBS-Triton with 2% BSA for two nights at 4°C. After extensive washes with TBS, we incubated the sections for 1 h at RT with horseradish peroxidase-conjugated anti-mouse secondary antibody (1:200) and for 1 h with avidin-biotin-peroxidase complex (1:200; ABC Kit, Vector Laboratories, Burlingame, CA, USA). Staining was visualized using 3,3′-diaminobenzidine (DAB) as chromogen. Sections were counterstained with thionine and coverslipped using Entellan (Merck Chemicals, Darmstadt, Germany).

Sections for *BBOX1* and *FARSA* were deparaffinized, rehydrated and washed in PBS followed by heat-induced antigen retrieval in citrate-buffer pH 6. Subsequently, the sections were depleted of neuromelanin using potassium permanganate, potassium metabisulfite and oxalic acid in order to evaluate the cellular localization. After the above-described antigen retrieval, sections were washed in TBS and incubated in rabbit polyclonal antibody against BBOX1 (1:100, HPA007600, Atlas Antibodies) or rabbit polyclonal antibody against FARSA (1:4000, HPA001911, Atlas Antibodies) diluted in TBS-Triton with 1% BSA and 5% normal donkey serum for 1 h at RT and two nights at 4°C. After extensive washes with TBS, sections were incubated in 0.3% hydrogen peroxide to eliminate endogenous peroxidase activity, again washed with TBS and incubated with horseradish peroxidase-conjugated secondary antibody for 1 h and an additional hour with ABC (Vector Laboratories). Staining was visualized using DAB and sections were dehydrated and coverslipped using Entellan. Negative control sections were treated identically, except for the primary antibody that was omitted. There was no immunostaining observed in these negative control sections. Photographs (200× and 630× magnification) were captured using a Leica microscope (LEICA DMR, Leica Microsystems BV, Rijswijk, The Netherlands) equipped with a CCD Microfire (Optronics, Goleta, CA, USA) color video camera using Neurolucida software version 9 (Microbrightfield Inc., Colchester, VT, USA).

RESULTS

Differential protein levels and pathogenetic pathways in the LC in PD

One-dimensional gel-electrophoresis of LC homogenates followed by in-gel tryptic digestion, nano-LC-FTMS/MS and database searching resulted in the identification of 2495 proteins. The overall protein profiles of the LC in PD patients and controls were very similar. Functional protein classification of all LC proteins using PANTHER classification indicated that the most represented functional classes were transferases (8.7% of 2495 proteins), nucleic acid binding proteins (8.6%), oxidoreductases (7.5%), enzyme modulators (7.1%) and transporters (7.1%). We refer to the supplementary material for the Coomassie Blue-stained protein gel images of LC lysates (Supporting Information Figure S1), the full list of identified proteins including the raw and normalized spectral counts (Supporting Information Table S1) and a pie chart of all represented functional protein classes (Supporting Information Figure S2).

Quantitative analysis of normalized protein spectral counts and statistical analysis yielded 87 proteins that had significantly different expression levels when comparing PD patients with controls, with 33 upregulated and 54 downregulated proteins (Table 2). We refer to Supporting Information Figure S3 for a heat map view of the cluster analysis using the differentially regulated proteins. Based on the GO annotation of cellular component (6), the differentially expressed proteins were predominantly localized in the cytoplasm (50.6%), cytosol (20.7%), mitochondrion (19.5%), membrane (general 19.5%; plasma membrane 18.4%; endoplasmic reticulum membrane 10.3%), nucleus (18.4%), endoplasmic reticulum (12.6%) or were attached to the membrane (17.2%). Note that the sum of percentages exceeds 100% because of multiple cellular components for certain proteins.

Sixty-one out of 87 differentially expressed proteins were associated with processes that have previously been implicated in the pathogenesis of PD (Figure 1). These included oxidative stress (11.5% of the 87 differentially expressed proteins), mitochondrial dysfunction (10.3%), cytoskeleton structure and regulation (10.3%), inflammation and glial activation (8%) and synaptic neurotransmission (6.9%).

Ingenuity pathway analysis of the differentially expressed proteins led to three significantly altered pathways: aminoacyl-tRNA-biosynthesis ($P = 0.005$), arginine and proline metabolism ($P = 0.005$) and phenylalanyl, tyrosine and tryptophan biosynthesis ($P = 0.005$). The aminoacyl-tRNA-biosynthesis pathway included isoform 1 of Rab3 GTPase-activating protein non-catalytic subunit (RAB3GAP2), cytoplasmic isoleucyl-tRNA synthetase (IARS), FARSA and phenylalanyl-tRNA synthetase beta chain (FARSB) whereas creatine kinase B-type (CKB), isoform 1 of nitric oxide synthase (NOS1), mitochondrial aldehyde dehydrogenase X (ALDH1B1), SAT2 protein (SAT2) and isoform 1 of cytosol aminopeptidase (LAP3) were involved in arginine and proline metabolism. The proteins implicated in phenylalanyl, tyrosine and tryptophan biosynthesis partly overlapped with the aminoacyl-tRNA-biosynthesis proteins: isoform alpha-enolase of alpha-enolase (ENO1), FARSA and FARSB.

Validation using Western blotting and immunohistochemistry

The expression of a selection of proteins was analyzed using both Western blotting and immunohistochemistry in order to confirm the direction of change of these proteins in PD patients compared with controls using a different, antibody-based approach (Figures 2 and 3; Supporting Information Figure S4). Proteins were selected for Western blotting and/or immunohistochemistry using the following criteria: (i) *P*-value lower than 0.05; (ii) positive or negative fold change equal to or higher than 2.0; and (iii) commercial availability of antibodies. From the 48 proteins that fulfilled these criteria, we selected both up- and downregulated proteins that were involved in different pathways. We furthermore took into account the quality of antibodies and selected antibodies that were specific for the detected isoform. The selected proteins were TH, FARSA, BBOX1, KTN1 and C4B.

Table 2. List of differentially expressed proteins in the locus ceruleus of PD patients compared with controls ranked on fold change. Abbreviations: IPI = International Protein Index; PD = Parkinson's disease.

Protein name	IPI number	Gene symbol	Fold change	*P*-value	Functional classification*
Dopamine beta-hydroxylase	IPI00171678	DBH	−∞	0.00014	Hydroxylase
Isoform 2 of ELAV-like protein 4	IPI00395507	ELAVL4	−∞	0.0040	mRNA processing factor
Isoform 1 of uncharacterized protein KIAA0513	IPI00028516	KIAA0513	−∞	0.0040	None
28S ribosomal protein S6, mitochondrial	IPI00305668	MRPS6	−∞	0.0073	Ribosomal protein
Serine/threonine-protein kinase Nek7	IPI00152658	NEK7	−∞	0.0086	Protein kinase
Putative uncharacterized protein MRPL23	IPI00658024	MRPL23	−∞	0.015	Ribosomal protein
7-dehydrocholesterol reductase	IPI00294501	DHCR7	−∞	0.016	Receptor
28S ribosomal protein S34, mitochondrial	IPI00169413	MRPS34	−∞	0.021	None
Galectin-3	IPI00465431	LGALS3	−∞	0.023	Signaling molecule
Isoform 2 of tyrosine 3-monooxygenase	IPI00218276	TH	−23.965	0.00013	Oxygenase
Neuroglobin	IPI00009758	NGB	−13.079	0.0030	Transporter
HESB like domain containing 2, isoform CRA_b	IPI00329615	ISCA1	−8.286	0.013	None
Probable E3 ubiquitin-protein ligase HERC1	IPI00022479	HERC1	−6.165	0.048	Chromatin/chromatin-binding protein
Resistance to inhibitors of cholinesterase 8 homolog A	IPI00100106	RIC8A	−5.577	0.048	None
Isoform 2 of serine/threonine-protein kinase PAK 3	IPI00027382	PAK3	−4.659	0.0046	Protein kinase
Isoform 2 of small G protein signaling modulator 1	IPI00514149	SGSM1	−4.623	0.045	Hydrolase
Isoform 1 of regulator of nonsense transcripts 1	IPI00034049	UPF1	−3.444	0.0018	DNA helicase
Thioredoxin domain-containing protein 4	IPI00401264	ERP44	−3.426	0.033	Isomerase
Gamma-aminobutyric acid receptor-associated protein	IPI00027253	GABARAP	−3.418	0.043	Non-motor microtubule binding protein
Carbonyl reductase [NADPH] 3	IPI00290462	CBR3	−3.352	0.048	Dehydrogenase
Brefeldin A-inhibited guanine nucleotide-exchange protein 3	IPI00514897	KIAA1244	−3.347	0.0011	Guanyl-nucleotide exchange factor
Rap guanine nucleotide exchange factor 2	IPI00853219	RAPGEF2	−2.984	0.042	Guanyl-nucleotide exchange factor
Isoleucyl-tRNA synthetase, cytoplasmic	IPI00644127	IARS	−2.954	0.015	Amino-acyl tRNA synthetase
Isoform 1 of nitric oxide synthase, brain	IPI00217225	NOS1	−2.842	0.037	Nuclease
Arginine-rich, mutated in early stage tumors	IPI00328748	MANF	−2.759	0.037	None
Coatomer subunit beta	IPI00295851	COPB1	−2.718	0.013	Vesicle coat protein
Isoform 1 of Rab3 GTPase-activating protein non-catalytic subunit	IPI00554590	RAB3GAP2	−2.539	0.0034	G-protein modulator
GrpE protein homolog 1, mitochondrial	IPI00029557	GRPEL1	−2.454	0.019	Cytoskeletal protein
Phenylalanyl-tRNA synthetase alpha chain	IPI00031820	FARSA	−2.432	0.0091	Amino-acyl tRNA synthetase
Isoform Long of cold shock domain-containing protein E1	IPI00470891	CSDE1	−2.239	0.041	None
Isoform 2 of protein tweety homolog 1	IPI00010183	TTYH1	−2.113	0.048	Anion channel
Protein FAM127A	IPI00816474	FAM127A	−2.104	0.011	None
Isoform 2 of ankyrin-3	IPI00472779	ANK3	−2.037	0.0061	Cytoskeletal protein
Isoform 1 of acyl-coenzyme A thioesterase 9, mitochondrial	IPI00220710	ACOT9	−2.006	0.0084	Esterase
Phospholipase D3	IPI00328243	PLD3	−1.983	0.038	Phospholipase
Isoform 1 of kinectin	IPI00328753	KTN1	−1.972	0.0012	Receptor
Dolichyl-diphosphooligosaccharide-protein glycosyltransferase subunit 1 precursor (Ribophorin I)	IPI00025874	RPN1	−1.910	0.020	Glycosyltransferase
LYR motif-containing protein 4	IPI00006979	LYRM4	−1.836	0.030	None
Tumor protein D52 isoform 2	IPI00619951	TPD52	−1.808	0.037	None
Isoform 1 of UDP-glucose: glycoprotein glucosyltransferase 1	IPI00024466	UGGT1	−1.790	0.015	Glycosyltransferase
Protein kinase, cAMP-dependent. regulatory, type II, alpha, isoform CRA_b	IPI00063234	PRKAR2A	−1.783	0.040	Kinase modulator
Flotillin-1	IPI00027438	FLOT1	−1.714	0.014	Membrane traffic protein
Seipin	IPI00479357	BSCL2	−1.683	0.014	None
FK506-binding protein 4	IPI00219005	FKBP4	−1.667	0.019	Isomerase
Phenylalanyl-tRNA synthetase beta chain	IPI00300074	FARSB	−1.655	0.018	Nucleic acid binding

Table 2. *Continued*

Protein name	IPI number	Gene symbol	Fold change	*P*-value	Functional classification*
Upregulated during skeletal muscle growth protein 5	IPI00063903	USMG5	−1.554	0.017	None
Prolow-density lipoprotein receptor-related protein 1	IPI00020557	LRP1	−1.537	0.043	Receptor
Isoform 1 of Mammalian ependymin-related protein 1	IPI00259102	EPDR1	−1.516	0.032	None
cDNA FLJ56389, highly similar to Elongation factor 1-gamma	IPI00000875	EEF1G	−1.352	0.030	Anion channel
A kinase (PRKA) anchor protein 12 isoform 2	IPI00217683	AKAP12	−1.265	0.011	None
Gamma-synuclein	IPI00297714	SNCG	−1.255	0.020	Signaling molecule
cDNA FLJ56034, highly similar to 4-aminobutyrate aminotransferase, mitochondrial	IPI00009532	ABAT	−1.249	0.0095	Transaminase
Isoform IA of synapsin-1	IPI00300568	SYN1	−1.208	0.034	Membrane trafficking regulatory protein
Leucine-rich PPR motif-containing protein, mitochondrial	IPI00783271	LRPPRC	−1.193	0.042	Transporter
Isoform alpha-enolase of alpha-enolase	IPI00465248	ENO1	1.152	0.049	Lyase
Isoform M1 of pyruvate kinase isozymes M1/M2	IPI00220644	PKM2	1.155	0.00060	Carbohydrate kinase
Creatine kinase B-type	IPI00022977	CKB	1.178	0.015	Amino acid kinase
gelsolin isoform c	IPI00647556	GSN	1.181	0.046	Non-motor actin binding protein
Carbonic anhydrase 2	IPI00218414	CA2	1.209	0.050	Dehydratase
Isoform V0 of Versican core protein	IPI00009802	VCAN	1.258	0.046	Extracellular matrix glycoprotein
Adenylate kinase isoenzyme 1	IPI00018342	AK1	1.277	0.033	Nucleotide kinase
Ferritin heavy chain	IPI00554521	FTH1	1.292	0.019	Storage protein
Protein-arginine deiminase type-2	IPI00294187	PADI2	1.337	0.0010	Hydrolase
Isoform 1 of cytosol aminopeptidase	IPI00419237	LAP3	1.355	0.018	Metalloprotease
Vimentin	IPI00418471	VIM	1.369	0.020	Structural protein
Inositol monophosphatase	IPI00020906	IMPA1	1.374	0.038	Phosphatase
V-crk sarcoma virus CT10 oncogene homolog isoform b	IPI00305469	CRK	1.926	0.016	None
Isoform 1 of regucalcin	IPI00017551	RGN	1.930	0.047	Esterase
Transgelin	IPI00216138	TAGLN	1.971	0.037	Non-motor actin binding protein
Gamma-butyrobetaine dioxygenase	IPI00027416	BBOX1	2.155	0.020	Hydroxylase
Ribosyldihydronicotinamide dehydrogenase [quinone]	IPI00219129	NQO2	2.191	0.046	None
HLA class I histocompatibility antigen, B-59 alpha chain	IPI00472073	HLA-B	2.987	0.0071	Immunoglobulin receptor family
Complement component 4B	IPI00887154	C4B	3.063	0.0078	None
Wolframin	IPI00008711	WFS1	3.373	0.015	None
Putative uncharacterized protein DKFZp686I04196 (Fragment)	IPI00399007	IGHG2	3.621	0.019	Immunoglobulin
c-Myc-responsive protein Rcl	IPI00007926	C6ORF108	4.234	0.048	None
cDNA FLJ55177, highly similar to ras-related protein Ral-B	IPI00004397	RALB	4.374	0.027	Small GTPase
Mitochondrial glutamate carrier 2	IPI00027826	SLC25A18	7.117	0.032	Amino acid transporter
Isoform 1 of NHL repeat-containing protein 2	IPI00301051	NHLRC2	7.357	0.024	None
Aldehyde dehydrogenase X, mitochondrial	IPI00103467	ALDH1B1	7.522	0.033	Dehydrogenase
Methylmalonyl-CoA epimerase, mitochondrial	IPI00107722	MCEE	7.905	0.012	DNA glycosylase
Isoform 2 of endoplasmic reticulum aminopeptidase 1	IPI00165949	ERAP1	9.501	0.020	Metalloprotease
SAT2 protein	IPI00744810	SAT2	∞	0.022	Acetyltransferase
Isoform 1 of catenin alpha-1	IPI00215948	CTNNA1	∞	0.021	Non-motor actin binding protein
Hemopexin	IPI00022488	HPX	∞	0.020	Transfer/carrier protein
Podocalyxin-like protein 1 precursor	IPI00299116	PODXL	∞	0.0083	None
HLA class II histocompatibility antigen, DRB1-1 beta chain	IPI00738107	HLA-DRB1	∞	0.0021	Major histocompatibility complex antigen

*According to functional PANTHER classification (http://www.pantherdb.org).

Figure 1. Listing of differentially expressed proteins associated with known pathogenetic pathways in Parkinson's disease (PD). Plus and minus signs indicate increased (+) or decreased (–) protein levels in PD patients compared with controls.

For all proteins analyzed, the Western blot data supported the results of the proteomic analysis: the levels of TH, FARSA, and KTN1 were decreased (TH −62% compared with controls, FARSA −23%, KTN1 −44%) whereas the levels of BBOX1 and C4B were increased in PD compared with controls (BBOX1 +85% compared with controls; C4B +88%; Figure 2). For TH ($P = 0.006$), KTN1 ($P = 0.01$) and C4B ($P = 0.01$) Western blot data were significantly different, P-values for FARSA ($P = 0.09$) and BBOX1 ($P = 0.08$) indicated a trend. The expression level of the reference protein actin was not significantly different between the PD and control
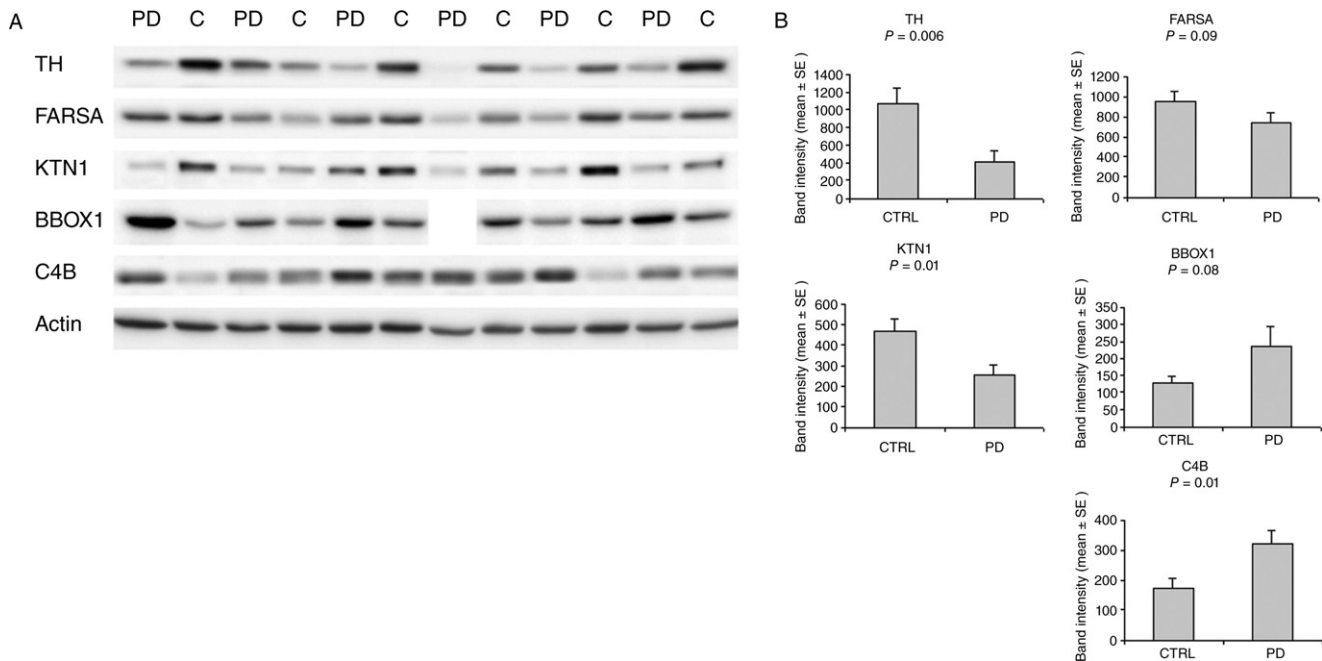
Figure 2. *Confirmation of proteomic candidates by Western blotting.* **A.** Western blots for the five proteins that were selected for technical validation. Actin was included as a control protein that should not change between samples. **B.** Bar graphs of average band intensities for the blotted proteins. Data for BBOX1 of the fourth PD patient from the left were excluded from quantitative analysis because of an artifact. Abbreviations: TH = tyrosine hydroxylase; FARSA = phenylalanyl-tRNA synthetase alpha chain; KTN1 = isoform 1 of kinectin; BBOX1 = gammabutyrobetaine dioxygenase; C4B = complement component 4B.
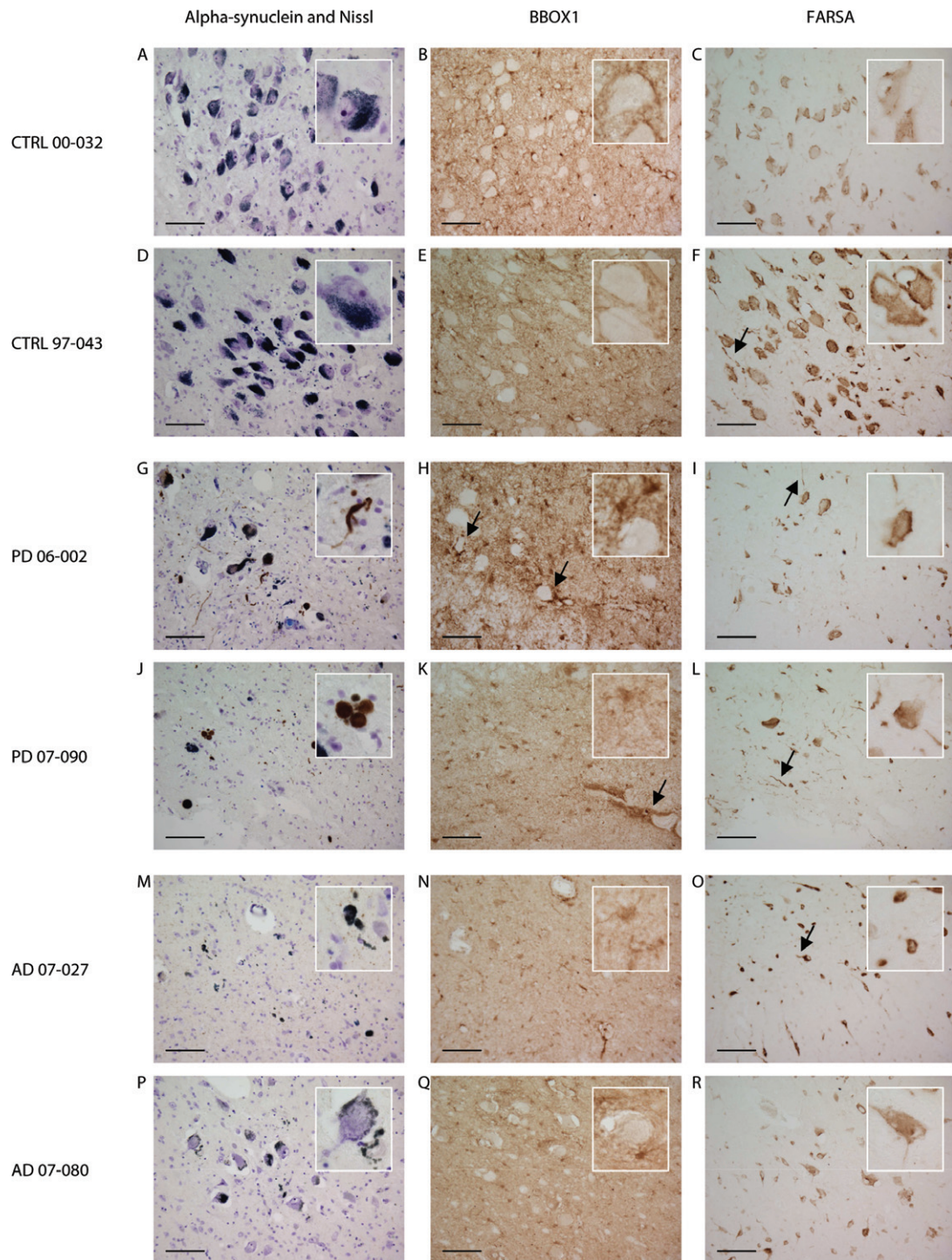
Figure 3. *Localization of phenylalanyl-tRNA synthetase alpha chain (FARSA) and gammabutyrobetaine dioxygenase (BBOX1) by immunohistochemistry in paraffin sections (10 μm) of the locus ceruleus of PD patients, controls and AD patients.* Alpha-synuclein and Nissl staining of the locus ceruleus (LC) of controls (**A,D**), PD patients (**G,J**) and AD patients (**M,P**) revealed neuronal loss in PD and AD patients and alpha-synuclein immunostained Lewy bodies and Lewy neurites in PD patients. BBOX1 was detected in both soma and cellular processes of glial cells of the LC of controls (**B,E**), PD patients (**H,K**) and AD patients (**N,Q**); arrows in picture H indicate BBOX1 staining surrounding LC neurons in a PD patient with relatively little cell death; enriched staining pattern in blood vessel endothelium is pointed out by arrow in picture **K**. In controls (**C,F**), PD (**I,L**) and AD patients (**O,R**) FARSA staining in the LC was localized in the cytoplasm and cellular processes of both neuronal and glial cells. In the cytoplasm of neurons, FARSA staining was diffuse and granular, predominantly near the cell borders and the nuclear membrane; arrows denote FARSA staining in a number of glial and neuronal processes. Scale bar = 1 μm.

group ($P = 0.44$). These data confirmed the proteomic data for cytoplasmic actin (fold-change PD compared with controls 1.07; $P = 0.27$).

Alpha-synuclein and Nissl stainings on the sections of all PD patients and none of the controls revealed alpha-synuclein-immunoreactive Lewy bodies and Lewy neurites and neuronal loss in the LC. Neuronal loss in the LC was also observed in all AD patients, although the degree of cell loss was highly variable. Lewy bodies and Lewy neurites were not seen in the LC of AD patients.

Microscopical examination of BBOX1 immunostaining revealed that this protein was localized in both soma and cellular processes of glial cells, but not in neurons, in the LC of PD patients, AD patients and controls (Figure 3B,E,H,K,N,Q).

BBOX1 staining in glial cells surrounding LC neurons was observed in PD cases with relatively little neuronal loss in the LC (as in Figure 3H). This staining pattern was less pronounced in PD cases with more extensive neuronal death and in all four AD cases (as in Figure 3K,N,Q). In contrast to the PD cases, we did not observe a relation between BBOX1 expression and the extent of neuronal loss in the AD cases. BBOX1 was furthermore enriched in blood vessel endothelium and ependymal cells in all cases (pointed out by arrow in Figure 3K).

FARSA was localized in the cytoplasm and cellular processes of both neuronal and glial cells in PD patients as well as AD cases and controls (Figure 3C,F,I,L,O,R). The number of FARSA-immunoreactive neurons in the LC of PD patients and AD patients was markedly decreased compared with the controls. Although localization in cellular processes was seen in all cases, including the controls, it appeared that this localization was more profound in PD and AD patients, which indicates that our findings for FARSA may not be specific for PD. The distribution of FARSA was diffuse and granular in the cytoplasm of neurons and appeared enriched near the cell membrane and the nuclear membrane.

DISCUSSION

By profiling protein expression of accurately dissected post-mortem LC tissue in PD patients and comparing with LC tissue of non-neurological controls, we aimed to identify proteins and processes that are involved in the pathogenesis of PD and to obtain new pathogenetic insights. To our knowledge this is the most comprehensive proteomic analysis of post-mortem PD brain tissue to date, and the first analysis of the human LC proteome. Until now, comparative proteomic analysis of human post-mortem tissue of PD patients had been restricted to substantia nigra and frontal cortical regions (7, 8, 25, 30, 49, 50, 56) and had largely been restricted to analysis of pooled patient samples (25, 30, 49, 50). Importantly, we analyzed a series of individual patient samples and matched controls. The most important finding of our study is that the LC proteome of PD patients not only reflects alterations in pathways and processes that were previously implicated in PD pathogenesis, most importantly mitochondrial dysfunction, oxidative stress and cytoskeletal dysregulation, but also reveals less known and hitherto unknown PD-related proteins and pathogenetic pathways, in particular aminoacyl-tRNA-biosynthesis.

The most significantly downregulated proteins in our dataset, TH and dopamine beta-hydroxylase (DBH) reflect the expected catecholaminergic neuronal loss in the LC of PD patients. Both proteins are enzymes involved in the synthesis of noradrenaline: TH is responsible for the conversion of tyrosine into L-dopa and DBH converts dopamine into noradrenaline.

Three mitochondrial ribosomal proteins—proteins that play a central role in translation within the mitochondrion (28)—were present in the top-10 list of downregulated proteins (see Table 1), which supports a pathogenetic role of mitochondrial dysfunction in PD (46): mitochondrial 28S ribosomal protein S6 (MRPS6), mitochondrial 28S ribosomal protein S34 (MRPS34) and mitochondrial ribosomal protein L23 (MRPL23). Interestingly, the gene encoding MRPS6, was previously identified in a gene expression study in post-mortem PD and control brains as a dysregulated gene in PD (39).

The mitochondrial protein ALDH1B1, as well as several other differentially regulated proteins in our dataset, including ferritin heavy chain (FTH1), catalyze oxidation-reduction reactions (6) that may link them with increased oxidative stress as previously observed in affected post-mortem brain tissue in PD (46). The increased levels of FTH1 were in agreement with previous proteomic and gene expression data of the substantia nigra (29, 56).

The most upregulated protein in our dataset was the DRB1-1 beta chain of HLA class II histocompatibility antigen (HLA-DRB1), which plays a central role in the immune response by antigen processing and presentation (6). Several other inflammatory molecular markers were increased in the LC of PD patients in our dataset including HLA class I HLA B-59 alpha chain (HLA-B) and C4B. Inflammation may be a non-specific secondary response to neuronal damage in the LC. As noradrenalin can suppress inflammation (19), the loss of noradrenergic neurons may contribute to increased levels of inflammatory markers. Inflammatory changes in the LC have been reported before, in particular mild astro- and microglia activation (10).

In the present study, we observed altered levels of three proteins that are responsible for protein degradation, a process that is impaired in PD (55). The levels of two aminopeptidases were increased in PD patients compared with controls: isoform 2 of endoplasmic reticulum aminopeptidase 1 (ERAP1) and LAP3. Aminopeptidases are high-abundant proteolytic enzymes in the brain (17) and altered plasma levels of cystine- and aspartate-aminopeptidases have previously been related to PD (18).

Several cytoskeletal proteins were dysregulated in our dataset, including ankyrin and vimentin. The elevated vimentin levels match with the higher vimentin gene expression previously observed in the PD substantia nigra (12, 29). We were furthermore intrigued by a more than fourfold decrease in the levels of the classic axon-guidance molecule serine/threonine-protein kinase PAK 3 (PAK3) in the LC of PD patients. Genome-wide association datasets indicate that this protein is associated with a genetic risk for PD (34).

A cytoskeleton-related protein that has not yet been described for PD is KTN1, which expression was decreased in our PD patients. KTN1 is an integral membrane protein primarily located in the endoplasmic reticulum (53) that binds to kinesin, a motor protein responsible for moving cellular components along microtubules in both axons and dendrites (54). The family of kinesins have previously been related to Alzheimer's and Huntington's disease (23). The possible involvement of the cytoskeleton in the pathogenesis of PD has also been put forward in recent proteomic studies on lymphocytes (35) and a PD cellular model (2).

Adding to alterations in cytoskeletal proteins, we also observed changes in proteins related to protein folding. Mitochondrial GrpE protein homolog 1 (GRPEL1), FK506-binding protein 4 (FKBP4), thioredoxin domain-containing protein 4 (ERP44) and isoform 1 of UDP-glucose:glycoprotein glucosyltransferase 1 (UGGT1) were all downregulated in the PD patients. These proteins play a role in protein folding either as a component of the Hsp70 or Hsp90 chaperone machinery (GRPEL1, FKBP4) (11, 32), as a endoplasmic reticulum folding assistant (ERP44) (4) or by reglucosylating unfolded glycoproteins (UGGT1) (52).

Interestingly, we also found differences in expression levels of proteins involved in cellular calcium homeostasis, including regucalcin and the transmembrane endoplasmic reticulum protein wolframin. Wolframin was previously linked with PD: a single-nucleotide polymorphism mutation in the gene that encodes wolframin was associated with a higher risk for the disease (47). According to our knowledge, regucalcin has not previously been linked with PD. Regucalcin plays a role in maintaining intracellular calcium homeostasis by activating Ca^{2+} pump enzymes (57). The general association between calcium and PD pathogenesis was suggested by the possible neuroprotective role of centrally acting L-type calcium channel blockers in PD (44).

In contrary to most other differentially expressed proteins in our dataset, isoform 2 of ELAV-like protein 4 (ELAVL4), which was detected in five out of six controls, but in none of the PD patients, could not be related to a known pathogenetic pathway. ELAVL4 is an mRNA binding protein and implicated in neuronal differentiation and maintenance (16). Genetic variants of ELAVL4 have been associated with the risk for PD (16, 22) and its age of onset (33, 38).

Finally, it is noteworthy to address the expression of the protein alpha-synuclein, which is a major component of Lewy bodies. Alpha-synuclein expression levels in the LC of PD patients were not different from the controls in our dataset. The literature has been contradictory on the total amounts of alpha-synuclein in affected regions in PD patients compared with controls [reviewed in (51)]. A recent large post-mortem study on alpha-synuclein expression in PD, MSA and progressive supranuclear palsy indicated increased levels of membrane-associated alpha-synuclein in PD patients compared with controls, whereas the levels in the cytosolic fraction were normal (51).

In total, 70% of the differentially expressed proteins could be related to processes that have previously been implicated in the pathogenesis of PD. However, our pathway analysis did not detect significant alterations in these pathways. This may be explained by the small number of cases in combination with using conservative statistics, that is, P-values of the pathways were adjusted under B-H multiple testing corrections. Not correcting for multiple measurements did yield several previously implicated processes, including processes involved in energy metabolism and inflammation, such as pyruvate metabolism ($P = 0.007$), glycolysis/gluconeogenesis ($P = 0.01$) and the antigen presentation pathway ($P = 0.02$).

After multiple testing corrections, we detected significant alterations in three molecular pathways: (i) aminoacyl-tRNA-biosynthesis; (ii) arginine and proline metabolism; and (iii) phenylalanyl, tyrosine and tryptophan biosynthesis. All three pathways are implicated in the amino-acid cycle. Two of these pathways were reported in a PD gene expression study (12): aminoacyl-tRNA-biosynthesis was one of the several significantly altered gene

groups in the substantia nigra, and the expression of genes related to arginine and proline metabolism was altered in the putamen of PD patients compared with controls.

In our study, the expression levels of three aminoacyl-tRNA-synthetases (ARS) of the aminoacyl-tRNA-biosynthesis pathway were significantly different: FARSA, FARSB and IARS. ARS are enzymes responsible for the first step of protein synthesis; they join amino acids to their cognate tRNAs (5, 40). Several ARSs, however, do have secondary functions unrelated to tRNA charging including transcription, translation, inflammation and apoptosis [reviewed in (5, 40)]. The ARSs are responsible for incorporation of the correct amino acids in proteins. Mouse studies have demonstrated that incorporation of the wrong amino acid results in misfolded or unfolded proteins, protein accumulation and cell death (31), which provides a possible pathogenetic link between ARSs and protein aggregation in PD. Consequently, our data suggest involvement of ARS in the pathogenesis PD. The biological basis of the alterations of ARS expression levels in the LC in PD remains to be evaluated in future studies.

Proteomic data of earlier comparative proteomic analyses of human PD post-mortem brain tissue show little overlap with the 87 individual altered proteins in our dataset: 14 of these proteins were also differently expressed in previous proteomic studies involving PD substantia nigra and PD frontal cortex brain tissue (7, 8, 25, 30, 49, 50, 56) such as FTH1 (56), pyruvate kinase (25, 49) (PKM2) and gamma-synuclein (49) (SNCG). A similar low concordance was also seen between other studies [reviewed in (15)]. However, the molecular pathways wherein these proteins are involved do overlap between studies and include mitochondrial dysfunction and oxidative stress. The lack of similarity between the individual proteins in the various tissue proteomics studies can be explained by the analysis of different brain regions and by differences in the fractions of the regions that were analyzed, for example, mitochondrial, nuclear or cytosolic fractions vs. whole brain tissue lysates. An alternative explanation is the use of a diversity of techniques, each with its own detection and resolution properties (15).

It may be argued that the alterations of protein expression observed in this study may be secondary to the loss of catecholaminergic neurons in the LC of PD patients, as the average loss of catecholaminergic neurons in this region is around 70% in post-mortem brain tissue (10). This particularly applies to neuronal proteins of which the levels are decreased in PD, including DBH and TH that are both normally highly abundant in noradrenergic LC neurons and the proteins that cluster with DBH and TH, such as galectin-3 (LGALS3) and UGGT1. On the other hand, it is quite possible that neuronal proteins that were not significantly different in our dataset actually have increased expression levels inside neurons that are masked by the lower number of neurons in the total sample.

It has been reported that a selection of proteins repeatedly appears on lists of differentially expressed proteins in proteomic analyses (41). Three out of a recently published top 15 list of most reported differentially expressed proteins in human proteomic studies of total cellular homogenates overlap with our dataset (41). The proteins include alpha-enolase, pyruvate kinase M1/M2 and vimentin. Most probably, these proteins represent a general cellular stress response rather than a specific PD-related pathogenetic process.

The immunohistochemical validation of FARSA and BBOX1 provides some explanation for the changed levels of these proteins.

The immunohistochemical validation of FARSA suggests that lower levels of FARSA may be related to the reduced number of neurons in the LC, although increased amounts of glial cells in PD may partly compensate for the lower levels of neuronal FARSA. On the other hand, the localization of FARSA appeared to be more often present in the cellular processes in PD patients compared with controls, which may reflect a role in PD pathogenesis. A different localization of ARSs was previously observed for tyrosyl-tRNA-synthetase (YARS): in cell cultures expressing mutant YARS proteins, granular YARS immunoreactive structures were homogeneously distributed in most cells, in contrast to the preferential sorting to neuronal tips in non-mutant cells (26). AD patients revealed an expression pattern of FARSA that was similar to the PD patients indicating that the findings for PD were not specific.

Immunohistochemical validation of BBOX1 showed that increased glia activation may explain the increased levels of this protein in the LC of PD patients. This glia activation was less pronounced in the AD patients, although the small number of patients makes it difficult to draw firm conclusions.

It remains unclear whether changes in FARSA and BBOX1 and other differentially expressed proteins are the consequence or actually the cause of neuronal loss or glial activation. One way to take away the influence of protein alterations caused by cell death is to analyze microdissected neurons. However, the full biological significance of the changes in the LC proteome in PD as well as the specificity of our findings relative to other neurodegenerative disorders can only be established in future functional studies.

Conclusion

The aim of this study was to identify proteins and processes in the human post-mortem LC that are relevant to PD pathogenesis in order to obtain novel pathogenetic insights. We have demonstrated that the proteome of the affected LC: (i) reflects the main known molecular pathogenetic pathways in PD, most importantly mitochondrial dysfunction, oxidative stress and cytoskeleton dysregulation; (ii) emphasizes a potential pathogenetic role for previously identified candidate proteins such as the classic axon-guidance molecule serine/threonine protein kinase PAK3 and the mitochondrial ribosomal protein MRPS6; (iii) indicates a potential pathogenetic role for individual proteins that have not yet been associated with PD, such as the calcium-regulating protein regucalcin and the microtubule-associated protein KTN1; and (iv) suggests a pathogenetic role for the amino acid cycle and for aminoacyl-tRNA-biosynthesis in particular. Further evaluation of the biological mechanisms underlying the observed alterations in protein expression levels and how they relate to protein aggregation and neuronal death may ultimately lead to new therapeutic targets and/or novel diagnostic biomarkers for PD.

FUNDING

ACKNOWLEDGMENTS

REFERENCES

1. Alafuzoff I, Ince PG, Arzberger T, Al-Sarraj S, Bell J, Bodi I *et al* (2009) Staging/typing of Lewy body related alpha-synuclein pathology: a study of the BrainNet Europe Consortium. *Acta Neuropathol* **117**:635–652.

2. Alberio T, Bossi AM, Milli A, Parma E, Gariboldi MB, Tosi G *et al* (2010) Proteomic analysis of dopamine and alpha-synuclein interplay in a cellular model of Parkinson's disease pathogenesis. *FEBS J* **277**:4909–4919.

3. Albrethsen J, Knol JC, Piersma SR, Pham TV, de Wit M, Mongera S *et al* (2010) Subnuclear proteomics in colorectal cancer: identification of proteins enriched in the nuclear matrix fraction and regulation in adenoma to carcinoma progression. *Mol Cell Proteomics* **9**:988–1005.

4. Anelli T, Alessio M, Mezghrani A, Simmen T, Talamo F, Bachi A *et al* (2002) ERp44, a novel endoplasmic reticulum folding assistant of the thioredoxin family. *EMBO J* **21**:835–844.

5. Antonellis A, Green ED (2008) The role of aminoacyl-tRNA synthetases in genetic diseases. *Annu Rev Genomics Hum Genet* **9**:87–107.

6. Ashburner M, Ball CA, Blake JA, Botstein D, Butler H, Cherry JM *et al* (2000) Gene ontology: tool for the unification of biology. The Gene Ontology Consortium. *Nat Genet* **25**:25–29.

7. Basso M, Giraudo S, Lopiano L, Bergamasco B, Bosticco E, Cinquepalmi A *et al* (2003) Proteome analysis of mesencephalic tissues: evidence for Parkinson's disease. *Neurol Sci* **24**:155–156.

8. Basso M, Giraudo S, Corpillo D, Bergamasco B, Lopiano L, Fasano M (2004) Proteome analysis of human substantia nigra in Parkinson's disease. *Proteomics* **4**:3943–3952.

9. Benarroch EE, Schmeichel AM, Low PA, Sandroni P, Parisi JE (2008) Loss of A5 noradrenergic neurons in multiple system atrophy. *Acta Neuropathol* **115**:629–634.

10. Bertrand E, Lechowicz W, Szpak GM, Dymecki J (1997) Qualitative and quantitative analysis of locus coeruleus neurons in Parkinson's disease. *Folia Neuropathol* **35**:80–86.

11. Borges JC, Fischer H, Craievich AF, Hansen LD, Ramos CH (2003) Free human mitochondrial GrpE is a symmetric dimer in solution. *J Biol Chem* **278**:35337–35344.

12. Bossers K, Meerhoff G, Balesar R, van Dongen JW, Kruse CG, Swaab DF *et al* (2009) Analysis of gene expression in Parkinson's disease: possible involvement of neurotrophic support and axon guidance in dopaminergic cell death. *Brain Pathol* **19**:91–107.

13. Braak H, Braak E (1991) Neuropathological staging of Alzheimer-related changes. *Acta Neuropathol* **82**:239–259.

14. Braak H, Del TK, Rub U, de Vos RA, Jansen Steur EN, Braak E (2003) Staging of brain pathology related to sporadic Parkinson's disease. *Neurobiol Aging* **24**:197–211.

15. Caudle WM, Bammler TK, Lin Y, Pan S, Zhang J (2010) Using "omics" to define pathogenesis and biomarkers of Parkinson's disease. *Expert Rev Neurother* **10**:925–942.

16. DeStefano AL, Latourelle J, Lew MF, Suchowersky O, Klein C, Golbe LI *et al* (2008) Replication of association between ELAVL4 and Parkinson disease: the GenePD study. *Hum Genet* **124**:95–99.

17. Duran R, Barrero FJ, Morales B, Luna JD, Ramirez M, Vives F (2010) Oxidative stress and plasma aminopeptidase activity in Huntington's disease. *J Neural Transm* **117**:325–332.

18. Duran R, Barrero FJ, Morales B, Luna JD, Ramirez M, Vives F (2011) Oxidative stress and aminopeptidases in Parkinson's disease patients with and without treatment. *Neurodegener Dis* **8**:109–116.

19. Galea E, Heneka MT, Dello RC, Feinstein DL (2003) Intrinsic regulation of brain inflammatory responses. *Cell Mol Neurobiol* **23**:625–635.

20. German DC, Manaye KF, White CL III, Woodward DJ, McIntire DD, Smith WK *et al* (1992) Disease-specific patterns of locus coeruleus cell loss. *Ann Neurol* **32**:667–676.

21. Gesi M, Soldani P, Giorgi FS, Santinami A, Bonaccorsi I, Fornai F (2000) The role of the locus coeruleus in the development of Parkinson's disease. *Neurosci Biobehav Rev* **24**:655–668.

22. Hicks AA, Petursson H, Jonsson T, Stefansson H, Johannsdottir HS, Sainz J *et al* (2002) A susceptibility gene for late-onset idiopathic Parkinson's disease. *Ann Neurol* **52**:549–555.

23. Hirokawa N, Niwa S, Tanaka Y (2010) Molecular motors in neurons: transport mechanisms and roles in brain function, development, and disease. *Neuron* **68**:610–638.

24. Hirsch EC, Hunot S (2009) Neuroinflammation in Parkinson's disease: a target for neuroprotection? *Lancet Neurol* **8**:382–397.

25. Jin J, Hulette C, Wang Y, Zhang T, Pan C, Wadhwa R *et al* (2006) Proteomic identification of a stress protein, mortalin/mthsp70/GRP75: relevance to Parkinson disease. *Mol Cell Proteomics* **5**:1193–1204.

26. Jordanova A, Irobi J, Thomas FP, Van DP, Meerschaert K, Dewil M *et al* (2006) Disrupted function and axonal distribution of mutant tyrosyl-tRNA synthetase in dominant intermediate Charcot-Marie-Tooth neuropathy. *Nat Genet* **38**:197–202.

27. Keller A, Nesvizhskii AI, Kolker E, Aebersold R (2002) Empirical statistical model to estimate the accuracy of peptide identifications made by MS/MS and database search. *Anal Chem* **74**:5383–5392.

28. Kenmochi N, Suzuki T, Uechi T, Magoori M, Kuniba M, Higa S *et al* (2001) The human mitochondrial ribosomal protein genes: mapping of 54 genes to the chromosomes and implications for human disorders. *Genomics* **77**:65–70.

29. Kim JM, Lee KH, Jeon YJ, Oh JH, Jeong SY, Song IS *et al* (2006) Identification of genes related to Parkinson's disease using expressed sequence tags. *DNA Res* **13**:275–286.

30. Kitsou E, Pan S, Zhang J, Shi M, Zabeti A, Dickson DW *et al* (2008) Identification of proteins in human substantia nigra. *Proteomics Clin Appl* **2**:776–782.

31. Lee JW, Beebe K, Nangle LA, Jang J, Longo-Guess CM, Cook SA *et al* (2006) Editing-defective tRNA synthetase causes protein misfolding and neurodegeneration. *Nature* **443**:50–55.

32. Li J, Richter K, Buchner J (2011) Mixed Hsp90-cochaperone complexes are important for the progression of the reaction cycle. *Nat Struct Mol Biol* **18**:61–66.

33. Li YJ, Scott WK, Hedges DJ, Zhang F, Gaskell PC, Nance MA *et al* (2002) Age at onset in two common neurodegenerative diseases is genetically controlled. *Am J Hum Genet* **70**:985–993.

34. Lin L, Lesnick TG, Maraganore DM, Isacson O (2009) Axon guidance and synaptic maintenance: preclinical markers for neurodegenerative disease and therapeutics. *Trends Neurosci* **32**:142–149.

35. Mila S, Albo AG, Corpillo D, Giraudo S, Zibetti M, Bucci EM *et al* (2009) Lymphocyte proteomics of Parkinson's disease patients reveals cytoskeletal protein dysregulation and oxidative stress. *Biomark Med* **3**:117–128.

36. Mirra SS, Heyman A, McKeel D, Sumi SM, Crain BJ, Brownlee LM *et al* (1991) The Consortium to Establish a Registry for Alzheimer's Disease (CERAD). Part II. Standardization of the neuropathologic assessment of Alzheimer's disease. *Neurology* **41**:479–486.

37. Nesvizhskii AI, Keller A, Kolker E, Aebersold R (2003) A statistical model for identifying proteins by tandem mass spectrometry. *Anal Chem* **75**:4646–4658.

38. Noureddine MA, Qin XJ, Oliveira SA, Skelly TJ, van der Walt J, Hauser MA *et al* (2005) Association between the neuron-specific RNA-binding protein ELAVL4 and Parkinson disease. *Hum Genet* **117**:27–33.

39. Papapetropoulos S, Ffrench-Mullen J, McCorquodale D, Qin Y, Pablo J, Mash DC (2006) Multiregional gene expression profiling identifies MRPS6 as a possible candidate gene for Parkinson's disease. *Gene Expr* **13**:205–215.

40. Park SG, Ewalt KL, Kim S (2005) Functional expansion of aminoacyl-tRNA synthetases and their interacting factors: new perspectives on housekeepers. *Trends Biochem Sci* **30**:569–574.

41. Petrak J, Ivanek R, Toman O, Cmejla R, Cmejlova J, Vyoral D *et al* (2008) Deja vu in proteomics. A hit parade of repeatedly identified differentially expressed proteins. *Proteomics* **8**:1744–1749.

42. Pham TV, Piersma SR, Warmoes M, Jimenez CR (2010) On the beta-binomial model for analysis of spectral count data in label-free tandem mass spectrometry-based proteomics. *Bioinformatics* **26**:363–369.

43. Piersma SR, Fiedler U, Span S, Lingnau A, Pham TV, Hoffmann S *et al* (2010) Workflow comparison for label-free, quantitative secretome proteomics for cancer biomarker discovery: method evaluation, differential analysis, and verification in serum. *J Proteome Res* **9**:1913–1922.

44. Ritz B, Rhodes SL, Qian L, Schernhammer E, Olsen JH, Friis S (2010) L-type calcium channel blockers and Parkinson disease in Denmark. *Ann Neurol* **67**:600–606.

45. Samuels ER, Szabadi E (2008) Functional neuroanatomy of the noradrenergic locus coeruleus: its roles in the regulation of arousal and autonomic function part I: principles of functional organisation. *Curr Neuropharmacol* **6**:235–253.

46. Schapira AH (2008) Mitochondria in the aetiology and pathogenesis of Parkinson's disease. *Lancet Neurol* **7**:97–109.

47. Shadrina M, Nikopensius T, Slominsky P, Illarioshkin S, Bagyeva G, Markova E *et al* (2006) Association study of sporadic Parkinson's disease genetic risk factors in patients from Russia by APEX technology. *Neurosci Lett* **405**:212–216.

48. Shevchenko A, Wilm M, Vorm O, Mann M (1996) Mass spectrometric sequencing of proteins silver-stained polyacrylamide gels. *Anal Chem* **68**:850–858.

49. Shi M, Jin J, Wang Y, Beyer RP, Kitsou E, Albin RL *et al* (2008) Mortalin: a protein associated with progression of Parkinson disease? *J Neuropathol Exp Neurol* **67**:117–124.

50. Shi M, Bradner J, Bammler TK, Eaton DL, Zhang J, Ye Z *et al* (2009) Identification of glutathione S-transferase pi as a protein involved in Parkinson disease progression. *Am J Pathol* **175**:54–65.

51. Tong J, Wong H, Guttman M, Ang LC, Forno LS, Shimadzu M *et al* (2010) Brain alpha-synuclein accumulation in multiple system atrophy, Parkinson's disease and progressive supranuclear palsy: a comparative investigation. *Brain* **133**:172–188.

52. Totani K, Ihara Y, Tsujimoto T, Matsuo I, Ito Y (2009) The recognition motif of the glycoprotein-folding sensor enzyme UDP-Glc:glycoprotein glucosyltransferase. *Biochemistry* **48**:2933–2940.

53. Toyoshima I, Yu H, Steuer ER, Sheetz MP (1992) Kinectin, a major kinesin-binding protein on ER. *J Cell Biol* **118**:1121–1131.

54. Vale RD (2003) The molecular motor toolbox for intracellular transport. *Cell* **112**:467–480.

55. van Dijk KD, Teunissen CE, Drukarch B, Jimenez CR, Groenewegen HJ, Berendse HW *et al* (2010) Diagnostic cerebrospinal fluid biomarkers for Parkinson's disease: a pathogenetically based approach. *Neurobiol Dis* **39**:229–241.

56. Werner CJ, Heyny-von HR, Mall G, Wolf S (2008) Proteome analysis of human substantia nigra in Parkinson's disease. *Proteome Sci* **6**:8.

57. Yamaguchi M (2005) Role of regucalcin in maintaining cell homeostasis and function (review). *Int J Mol Med* **15**:371–389.

58. Zweig RM, Cardillo JE, Cohen M, Giere S, Hedreen JC (1993) The locus ceruleus and dementia in Parkinson's disease. *Neurology* **43**:986–991.

SUPPORTING INFORMATION

Additional Supporting Information may be found in the online version of this article:

Figure S1. Coomassie Blue-stained protein gel images of locus ceruleus lysates. Precision Plus Protein standard (Bio-Rad Laboratories, Hercules CA, USA) was used as a reference marker. Abbreviations below the lanes correspond to subject numbers in Table 1: C1 = NBB00-032; C2 = NBB98-104; C3 = NBB95-101; C4 = NBB96-078; C5 = NBB03-013; C6 = NBB03-040; PD1 = NBB99-069; PD2 = NBB99-014; PD3 = NBB98-064; PD4 = NBB98-043; PD5 = NBB94-092; PD6 = NBB06-002.

Figure S2. Pie chart of functional protein classes of all identified proteins in the locus ceruleus using PANTHER classification. Numbers used in pie chart correspond to numbers in attached table.

Figure S3. Heat map view of supervised cluster analysis using the differentially expressed proteins. Supervised clustering of 87 proteins (horizontal axis) that had significantly different expression levels between PD patients (PD) and controls (CTRL; vertical axis), with 33 upregulated and 54 downregulated proteins. The colors indicate the protein abundances, which were normalized to zero mean and unit variance for each protein. NBB numbers correspond to subject numbers in Table 1.

Figure S4. Proteomic and Western blot data of individual PD patients and controls for proteins included in validation. Numbers on X-axis for PD patients and controls correspond to NBB subject numbers in Table 1. For proteomic data the normalized spectral counts are shown, for Western blot data the band intensity. Band intensity data for BBOX1 of PD patient 98-064 were excluded from quantitative analysis because of an artifact.

Table S1. List of all identified proteins and their raw and normalized spectral counts in the locus ceruleus of PD patients compared with controls sorted according to *P*-value. Spectral counts were normalized on the sum of the spectral counts per biological sample. NBB numbers correspond to subject numbers in Table 1; *IPI = International Protein Index.

Please note: Wiley-Blackwell are not responsible for the content or functionality of any supporting materials supplied by the authors. Any queries (other than missing material) should be directed to the corresponding author for the article.